



UNIVERSIDAD DE CHILE
FACULTAD DE CIENCIAS FÍSICAS Y MATEMÁTICAS
DEPARTAMENTO DE ASTRONOMÍA

**STUDY OF THE ROLE OF GAS IN THE FORMATION OF SMBH SEED,
THROUGH SIMULATIONS OF NSC WITH GAS EMBEDDED**

TESIS PARA OPTAR AL GRADO DE MAGÍSTER EN CIENCIAS, MENCIÓN
ASTRONOMÍA

BORIS CUEVAS GOMEZ

PROFESOR GUÍA:
Andrés Escala

MIEMBROS DE LA COMISIÓN:
PROFESOR 2
PROFESOR 3

Este trabajo ha sido parcialmente financiado por:
NOMBRE INSTITUCIÓN

SANTIAGO DE CHILE
2026

RESUMEN DE LA MEMORIA PARA OPTAR
AL TÍTULO DE MAGÍSTER EN CIENCIAS,
MENCIÓN ASTRONOMÍA
POR: BORIS CUEVAS GOMEZ
FECHA: 2026
PROF. GUÍA: ANDRÉS ESCALA

**STUDY OF THE ROLE OF GAS IN THE FORMATION OF SMBH SEED,
THROUGH SIMULATIONS OF NSC WITH GAS EMBEDDED**

Abstractd

*Una frase de dedicatoria,
pueden ser dos líneas.*

Saludos

Acknowledgments

Acknowledgments

Table of Contents

| | |
|--|-----------|
| 1. Introduction | 1 |
| 1.1. Formation Channels for SMBHs and the Collisional Paradigm | 1 |
| 1.2. The Role of Gas in Dense Stellar Systems | 1 |
| 1.3. Research Objectives and Thesis Outline | 1 |
| 2. Theoretical Framework | 2 |
| 2.1. Density criterion for stellar collisions | 2 |
| 2.2. Stars and gas in equilibrium | 2 |
| 3. Numerical Methods | 3 |
| 3.1. The AMUSE Framework | 3 |
| 3.2. N-body code: Ph4 | 3 |
| 3.2.1. Hermite integrator | 4 |
| 3.2.2. Block Time Steps | 5 |
| 3.2.3. Collisions and mergers | 6 |
| 3.2.4. Escaping stars | 7 |
| 3.3. SPH code: Fi | 8 |
| 3.3.1. Barnes-Hut tree | 8 |
| 3.3.2. Smoothed Particle Hydrodynamics | 9 |
| 3.4. Coupling strategy: Bridge | 10 |
| 4. Initial Conditions and Setup | 11 |
| 4.1. Stellar Cluster Models | 11 |
| 4.2. Gas Configurations | 11 |
| 4.3. Numerical Parameters | 11 |
| 5. Results and analysis | 12 |
| 5.1. Gas-Free Baseline Simulations | 12 |
| 5.2. Effects of Gas Fraction on Collision Rates | 12 |
| 5.3. Mass Spectrum Evolution and Massive Object Formation | 12 |
| 5.4. Comparative Analysis Across Gas Fractions | 12 |
| 6. Discussion and Conclusions | 13 |
| 6.1. Interpretation of Gas-Induced Enhancements | 13 |
| 6.2. Implications for SMBH Seed Formation | 13 |
| 6.3. Limitations and Future Work | 13 |
| References | 14 |

| | |
|--|-----------|
| Appendices | 15 |
| A. Fourth-Order Hermite Integration Scheme | 15 |
| A.1. Step 1: Particle selection | 15 |
| A.2. Step 2: Calculate the predicted position and velocities for all particles | 15 |
| A.3. Step 3: Calculate acceleration and jerk for particle i | 16 |
| A.4. Step 4: Second and third time derivative of acceleration, using Hermite interpolation | 16 |
| A.5. Step 5: Add corrections | 17 |
| A.6. Step 6: Time step update | 18 |

List of Figures

| | | |
|------|---|---|
| 3.1. | Schematic of the coupled numerical framework. The stellar N-body system (modelled with ph4) and the gaseous SPH system (modelled with Fi) interact gravitationally through the Bridge coupling scheme. | 3 |
| 3.2. | Representation of an oct tree | 9 |

Chapter 1

Introduction

- 1.1. Formation Channels for SMBHs and the Collisional Paradigm
- 1.2. The Role of Gas in Dense Stellar Systems
- 1.3. Research Objectives and Thesis Outline

Chapter 2

Theoretical Framework

2.1. Density criterion for stellar collisions

2.2. Stars and gas in equilibrium

Chapter 3

Numerical Methods

3.1. The AMUSE Framework

This thesis investigates the role of gas in the formation of supermassive black hole (SMBH) seeds via stellar collisions in dense clusters. In contrast with other works, we do not take into account gas accretion by stars, since we are interested exclusively in the gravitational interaction between gas and stars.

We require, in principle, three codes: 1) an N-body code to model the stellar dynamics, 2) a smoothed particle hydrodynamics (SPH) code to simulate the gas thermodynamics and self-gravity, and 3) a coupling scheme to manage the mutual gravitational interaction between these two components.

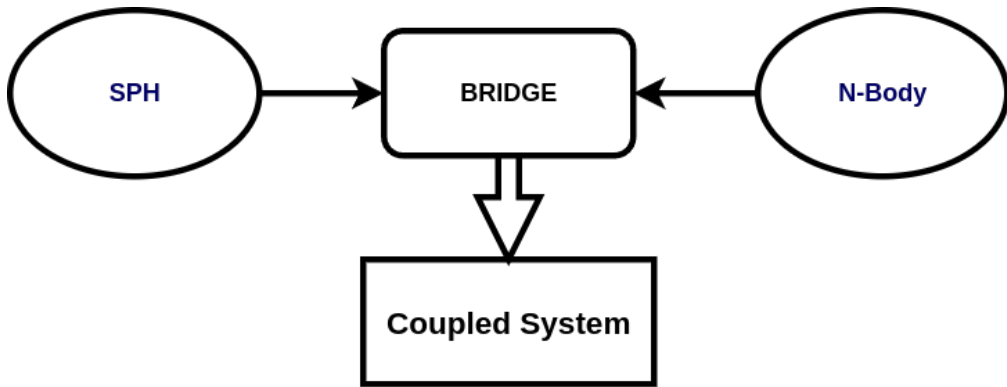


Figure 3.1: Schematic of the coupled numerical framework. The stellar N-Body system (modelled with `ph4`) and the gaseous SPH system (modelled with `Fi`) interact gravitationally through the `Bridge` coupling scheme.

The N-Body and SPH codes are accessed through the AMUSE interface (Zwart and McMillan, 2018), and coupled via an external code.

3.2. N-body code: Ph4

The proposed scenarios presented in (referencia a capitulo) require high numerical precision to accurately model close encounters and direct collisions. We therefore employ the `ph4` N-body code from the AMUSE framework (Zwart and McMillan, 2018).

In this section, we include a description of the code, and some external routines.

3.2.1. Hermite integrator

The Ph4 code uses a fourth-order Hermite integrator (Makino and Aarseth, 1992) for calculating the positions and velocities of stars due to gravity. This is a predictor-corrector method.

The fourth-order Hermite scheme is based on a precise calculation of the individual time step. Considering the particle i with its own time t_i , time step Δt_i , position \mathbf{x}_i , velocity \mathbf{v}_i , acceleration \mathbf{a}_i and jerk $\dot{\mathbf{a}}_i$, all calculated at time t_i . The integration algorithm proceeds as follows:

1. Select the particle with the minimum $t_i + \Delta t_i$. Set the global time to $t = t_i + \Delta t_i$.
2. Calculate the predicted positions (\mathbf{x}_p) and velocities (\mathbf{v}_p) for all particles, using the current values for \mathbf{x} , \mathbf{v} , \mathbf{a} , $\dot{\mathbf{a}}$.
3. Calculate the acceleration (\mathbf{a}_i) and jerk ($\dot{\mathbf{a}}_i$) for particle i at time $t_i + \Delta t_i$ using the predicted positions and velocities.
4. Calculate the second and third time derivatives of acceleration ($\mathbf{a}_i^{(2)}$ and $\mathbf{a}_i^{(3)}$) using Hermite interpolation.
5. Apply corrections to the position and velocity of particle i .
6. Calculate and update the time step Δt_i .
7. Repeat the algorithm.

A detailed derivation of the algorithm and the full set of equations are provided in Appendix A. From Eqs. (A.2) and (A.3), the predicted positions and velocities are:

$$\mathbf{x}_{p,j} = \mathbf{x}_j + \mathbf{v}_j(t - t_j) + \frac{\mathbf{a}_{0,j}}{2}(t - t_j)^2 + \frac{\dot{\mathbf{a}}_{0,j}}{3!}(t - t_j)^3 \quad (3.1)$$

$$\mathbf{v}_{p,j} = \mathbf{v}_j + \mathbf{a}_{0,j}(t - t_j) + \frac{\dot{\mathbf{a}}_{0,j}}{2!}(t - t_j)^2 \quad (3.2)$$

Here, \mathbf{x}_j and \mathbf{v}_j are the position and velocity of particle j at time t_j . The current acceleration $\mathbf{a}_{0,j}$ and jerk $\dot{\mathbf{a}}_{0,j}$ are computed as:

$$\mathbf{a}_{0,j} = \sum_{k \neq j} Gm_k \frac{\mathbf{r}_{0,jk}}{(\mathbf{r}_{0,jk}^2 + \epsilon^2)^{3/2}} \quad (3.3)$$

$$\dot{\mathbf{a}}_{0,j} = \sum_{k \neq j} Gm_k \left[\frac{\mathbf{v}_{0,jk}}{(\mathbf{r}_{0,jk}^2 + \epsilon^2)^{3/2}} - \frac{3(\mathbf{v}_{0,jk} \cdot \mathbf{r}_{0,jk})\mathbf{r}_{0,jk}}{(\mathbf{r}_{0,jk}^2 + \epsilon^2)^{5/2}} \right] \quad (3.4)$$

$$\mathbf{r}_{0,jk} = \mathbf{r}_k - \mathbf{r}_j \quad (3.5)$$

$$\mathbf{v}_{0,jk} = \mathbf{v}_k - \mathbf{v}_j \quad (3.6)$$

Using Hermite interpolation, the second and third time derivatives of the acceleration can be estimated. This estimation is subsequently used to correct the positions and velocities. The relevant expressions, derived in the appendix, are:

$$\mathbf{a}_{0,i}^{(2)} = \frac{-6(\mathbf{a}_{0,i} - \mathbf{a}_{1,i}) - \Delta t_i(4\dot{\mathbf{a}}_{0,i} + 2\ddot{\mathbf{a}}_{1,i})}{\Delta t_i^2} \quad (3.7)$$

$$\mathbf{a}_{0,i}^{(3)} = \frac{12(\mathbf{a}_{0,i} - \mathbf{a}_{1,i}) + 6(\dot{\mathbf{a}}_{0,i} + \dot{\mathbf{a}}_{1,i})\Delta t_i}{\Delta t_i^3} \quad (3.8)$$

The final corrected position and velocity of particle i are then given by:

$$\mathbf{x}_i(t_i + \Delta t_i) = \mathbf{x}_{p,i} + \frac{\mathbf{a}_{0,i}^{(2)} \Delta t_i^4}{24} + \frac{\mathbf{a}_{0,i}^{(3)} \Delta t_i^5}{120} \quad (3.9)$$

$$\mathbf{v}_i(t_i + \Delta t_i) = \mathbf{v}_{p,i} + \frac{\mathbf{a}_{0,i}^{(2)} \Delta t_i^3}{6} + \frac{\mathbf{a}_{0,i}^{(3)} \Delta t_i^4}{24} \quad (3.10)$$

These corrections incorporate terms up to fourth order. The main advantage of this method is that it only requires the explicit calculation of the acceleration and jerk at each step, with higher-order derivatives being obtained through the interpolation scheme.

3.2.2. Block Time Steps

An important part of the Hermite integrator is the time step calculation. The time step controls precision, energy conservation and integration time. While time steps are individual (each particle has its own), they are grouped into blocks for efficiency.

Time steps are set in two steps. First, a dynamic time step is calculated. Then, the time step is assigned using a block scheme. For the dynamical time step, the standard formula (A.35) is used:

$$\Delta t_i = \sqrt{\eta \frac{|\mathbf{a}_{1,i}| |\mathbf{a}_{1,i}^{(2)}| + |\dot{\mathbf{a}}_{1,i}|^2}{|\dot{\mathbf{a}}_{1,i}| |\mathbf{a}_{1,i}^{(3)}| + |\mathbf{a}_{1,i}^{(2)}|^2}} \quad (3.11)$$

As can be seen, $\mathbf{a}_{1,i}$ and $\dot{\mathbf{a}}_{1,i}$ are calculated in each step, while $\mathbf{a}_{1,i}^{(3)}$ is constant. Only $\mathbf{a}_{1,i}^{(2)}$ needs to be estimated:

$$\mathbf{a}_{1,i}^{(2)} = \mathbf{a}_{0,i}^{(2)} + \Delta t_i \mathbf{a}_{1,i}^{(3)} \quad (3.12)$$

When the simulation begins, the initial time steps are calculated using (A.37):

$$\Delta t = \eta_s \frac{|\mathbf{a}|}{|\dot{\mathbf{a}}|} \quad (3.13)$$

The main algorithm of the Hermite 4th-order scheme evolves the particle with the minimum $t_j + \Delta t_j$. As it is expensive to evolve particles one by one, the goal is to assign particles to discrete time steps. In Ph4, time steps are set to powers of two of the N-body time units.

During initialization, the time step is calculated using Equation (3.13), and then set. Given the initial time step $\Delta t_{0,j}$, the N-body time τ , and an integer n :

$$0.5 < \frac{\tau^{2^n}}{\Delta t_{0,j}} < 1 \quad (3.14)$$

The time step is then set to τ^{2^n} , with n being able to be positive or negative.

As the model evolves, the new time step is computed using (3.11). The time step is halved if the calculated time step is smaller than the current time step, and doubled if it is larger than twice the current time step.

The advantage of this time step criterion is that the time step in the code is equal to or lower than that required by the dynamics. Moreover, since particles share the same time steps, they can be integrated simultaneously. Additionally, all particles can be synchronized, as their times are multiples of powers of two of the same time unit.

3.2.3. Collisions and mergers

Stellar collisions occur in two steps. First, the collision is detected by the AMUSE routines in PH4, and then it is handled externally. PH4 has support for stopping conditions, specifically for collision detection.

All particles in AMUSE have different properties: position, velocity, mass, radius, among others. When `collision_detection` is enabled in PH4, the first filter is to check if two particles are closer than the sum of their radii:

$$|\Delta\mathbf{x}| < r_i + r_j \quad (3.15)$$

where $\Delta\mathbf{x}$ is the relative position vector between particles i and j , and r_i, r_j their respective radii. A second filter then verifies close encounters:

$$\epsilon |\Delta\mathbf{x}| |\Delta\mathbf{v}| > \Delta\mathbf{x} \cdot \Delta\mathbf{v} \quad (3.16)$$

where $\Delta\mathbf{v}$ is the relative velocity vector and $\epsilon = 0.001$. This avoids cases where particle superposition results from hyperbolic encounters with predominantly tangential relative velocities.

The stopping conditions allow the user to implement custom handling routines. For these simulations, we simply conserve linear momentum. When `collision_detection` is triggered, the code modifies the properties of one particle (preferentially the more massive one), setting its mass to the sum of the masses, its position to the center of mass, its velocity to the center-of-mass velocity, and its radius to conserve mass density:

$$m_{\text{new}} = m_i + m_j \quad (3.17)$$

$$\mathbf{x}_{\text{new}} = \frac{m_i \mathbf{x}_i + m_j \mathbf{x}_j}{m_i + m_j} \quad (3.18)$$

$$\mathbf{v}_{\text{new}} = \frac{m_i \mathbf{v}_i + m_j \mathbf{v}_j}{m_i + m_j} \quad (3.19)$$

$$r_{\text{new}} = r_i \left(\frac{m_i + m_j}{m_i} \right)^{1/3} \quad (3.20)$$

$$(3.21)$$

Finally, the other particle is removed from the simulation.

3.2.4. Escaping stars

After each analysis time step, potential escapers are identified through a multi-stage detection algorithm. To maintain mass and energy conservation, escaped stars are not removed from the simulation. Instead we add an extra attribute, `escaped` (all stars begin with `particles.escaped = False`), to track bound and unbound stars for subsequent analysis. The process begins with defining an appropriate length scale.

During initialization, the escape scale is defined as the minimum between ten times the virial radius and the Lagrangian radius containing the total mass:

$$r_{0,\text{esc}} = \min(10 \times r_{\text{vir}}, r_{100}) \quad (3.22)$$

where r_{100} represents the Lagrangian radius containing the total stellar mass. In subsequent iterations, the escape distance is updated as:

$$r_{\text{esc}} = \max(r_{\text{esc}}, 10 \times r_{b,\text{vir}}) \quad (3.23)$$

where $r_{b,\text{vir}}$ denotes the virial radius of bound stars.

The escape detection algorithm, executed at each time step, proceeds as follows:

1. Compute the core center and identify stars beyond the escape radius
2. Select gravitationally unbound stars
3. Identify stars with outward radial motion
4. Verify minimal gravitational influence on nearest neighbors

The core center location is determined using a density-weighted scheme following Sweatman (1993). For each star, the distance to its 7th nearest neighbor ($r_{i,7}$) is computed, and the density center is calculated as:

$$\mathbf{x}_c = \frac{\sum_{i=1}^N \mathbf{x}_i / r_{i,7}^3}{\sum_{i=1}^N 1 / r_{i,7}^3} \quad (3.24)$$

This formulation resembles a center of mass calculation but uses local stellar density instead of mass. Stars satisfying the condition

$$|\mathbf{x}_i - \mathbf{x}_c| > r_{\text{esc}} \quad (3.25)$$

are identified as potential escapers.

Gravitational unbinding is evaluated using the total energy $E_i = E_{p,i} + E_{k,i}$, where $E_{p,i}$ is the gravitational potential energy (including contributions from both stars and gas) and $E_{k,i}$ is the kinetic energy. Stars with $E_i \leq 0$ are considered bound, while those with $E_i > 0$ are classified as unbound. Among unbound stars, outward-moving candidates are identified through the condition:

$$\Delta \mathbf{x}_i \cdot \Delta \mathbf{v}_i > 0 \quad (3.26)$$

where $\Delta \mathbf{x}_i = \mathbf{x}_i - \mathbf{x}_c$ and $\Delta \mathbf{v}_i = \mathbf{v}_i - \mathbf{v}_c$ represent position and velocity relative to the cluster center. Similar to (3.24), the velocity of the core center is computed as

$$\mathbf{v}_c = \frac{\sum_{i=1}^N \mathbf{v}_i m_i / r_{i,7}^3}{\sum_{i=1}^N m_i / r_{i,7}^3} \quad (3.27)$$

The final validation step quantifies the gravitational influence on neighboring stars. For each candidate escaper, the relative potential energy ($e_{p,i}$) and kinetic energy ($e_{k,i}$) with respect to its nearest neighbor are computed. The energy ratio is defined as:

$$X_E := \frac{|e_{p,i}|}{e_{k,i}} \quad (3.28)$$

Stars satisfying $X_E < 0.01$ are confirmed as escapers, ensuring minimal gravitational perturbation to neighboring stars. These stars are tagged as escapers (`particles.escaped = True`).

3.3. SPH code: Fi

The gas dynamics are modelled using the **Fi** code (Gerritsen et al., 1997), an MPI-parallel smoothed particle hydrodynamics (SPH) implementation within the AMUSE framework. We focus on the aspects most relevant to our simulations; a comprehensive description of the code can be found in (Pelupessy, 2005).

3.3.1. Barnes-Hut tree

A key feature of **Fi** is its ability to compute the self-gravity of the gaseous component. Particle-based codes offer a range of methods for gravitational force calculation. The most accurate approach is the direct summation of all pairwise interactions, which scales as $\mathcal{O}(N^2)$ and is computationally expensive for large N . While such precision is often necessary for collisional stellar dynamics (e.g., in our N-body component), the gas system in our simulations is treated as a collisionless fluid for the purpose of gravity calculation, allowing for faster, approximate methods, sacrificing accuracy for computational efficiency.

Fi employs the Barnes-Hut (BH) tree algorithm (Barnes and Hut, 1986). This method uses a hierarchical oct-tree spatial decomposition and a geometric opening criterion to approximate gravitational forces.

The tree is constructed by enclosing all particles within a root cell. If this cell contains more than one particle, it is subdivided into eight daughter cells of equal volume. This subdivision process repeats recursively for each cell containing multiple particles, until every cell holds at most one particle (a leaf node). Figure 3.2 illustrates this structure in two dimensions.

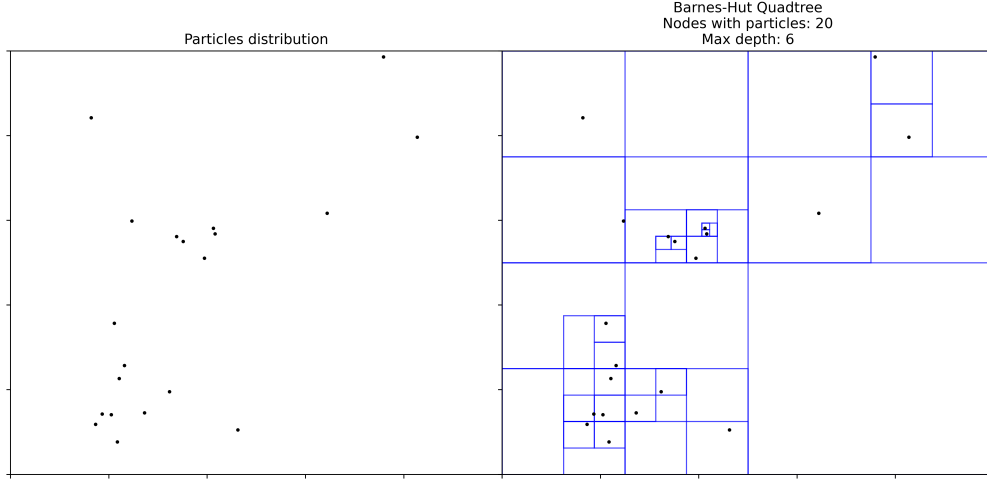


Figure 3.2: Representation of an oct tree

Once the tree is built, the gravitational force on a given particle is calculated by going through the tree from the root. For each node encountered (linked to a cell), a decision is made: either open the node to examine its children, or accept the node as a single interacting entity. The classic Barnes-Hut opening criterion is:

$$l/d < \theta \quad (3.29)$$

where l is the side length of the cubic cell, d is the distance from the target particle to the node's center of mass, and θ is an accuracy parameter. If this condition is met, the entire mass of the node is treated as a single point mass at its center of mass, providing an acceptable approximation when the node is sufficiently distant (i.e., appears small in angular size). The recursion stops upon reaching a leaf node, which by definition represents a single particle and is interacted with directly. This approximation reduces the computational cost of the force calculation from $\mathcal{O}(N^2)$ to $\mathcal{O}(N \log N)$ and adapts efficiently to clustered mass distributions, making it suitable for collisionless systems (Barnes and Hut, 1986).

The standard geometric criterion (Eq. 3.29), however, can fail in some circumstances (Salmon and Warren, 1994). Therefore, Fi implements a modified criterion following (Springel and Hernquist, 2002):

$$M_n l^4 < \alpha |\mathbf{a}| d^6 \quad (3.30)$$

where M_n is the total mass contained in the node, \mathbf{a} is an estimate of the gravitational acceleration (typically from the previous timestep), and α is a parameter to control accuracy.

3.3.2. Smoothed Particle Hydrodynamics

The gas dynamics are solved using the Smoothed Particle Hydrodynamics method (Gingold and Monaghan, 1977; Lucy, 1977). In SPH, hydrodynamic equations are solved from a Lagrangian approach, sampling the gas by a discrete set of points, instead of the classical continuous. Consider a gas described by density ρ , pressure p and specific internal energy u . For an inviscid fluid, the Lagrangian take the form:

$$L = \int \left\{ \frac{1}{2} v^2 - u[\rho(\mathbf{r})] \right\} \rho d^3 \mathbf{x} \quad (3.31)$$

where the specific internal energy is related to the pressure by $\partial u / \partial \rho = p / \rho^2$, and the position vector is $\mathbf{r} = (\mathbf{x}_1, \mathbf{x}_2, \mathbf{x}_3)$. The Euler equations of motion can be derived from a variational principle in the Lagrangian (Rasio, 2000):

$$\frac{\partial \rho}{\partial t} + \nabla \cdot (\rho \vec{v}) = 0 \quad (3.32)$$

$$\frac{\partial \vec{v}}{\partial t} + (\vec{v} \cdot \nabla) \vec{v} = - \frac{\nabla p}{\rho} \quad (3.33)$$

$$\frac{\partial u}{\partial t} + (\vec{v} \cdot \nabla) u = - \frac{p}{\rho} (\nabla \cdot \vec{v}) \quad (3.34)$$

where (3.32) is the equation of continuity, (3.33) is the equation of motion and (3.34) is the internal energy equation. In SPH, instead of (3.31), a discrete Lagrangian is used:

$$L_{SPH} = \sum_{i=1}^N m_i \left[\frac{1}{2} v_i^2 - u(\rho_i) \right] \quad (3.35)$$

where m_i , v_i , ρ_i are the mass, velocity and density of each particle, which represent a fluid element. In order to use (3.35) as the Lagrangian of the system, is necessary to use a suitable expression for the density.

In SPH, the density at position \mathbf{r} is calculated as an average over all particles:

$$\rho(\mathbf{r}) = \sum_i m_i W(\mathbf{r} - \mathbf{r}_i; h) \quad (3.36)$$

where $W(\mathbf{r} - \mathbf{r}_i; h)$ is a smoothing kernel of width h . The kernel has to fulfill two conditions: his integral over space should be unity and that in the limit $h \rightarrow 0$ approach to Dirac delta function. Note that with the first constrain, the integration of (3.36) gives the total mass of the system.

3.4. Coupling strategy: Bridge

Chapter 4

Initial Conditions and Setup

4.1. Stellar Cluster Models

4.2. Gas Configurations

4.3. Numerical Parameters

Chapter 5

Results and analysis

- 5.1. Gas-Free Baseline Simulations
- 5.2. Effects of Gas Fraction on Collision Rates
- 5.3. Mass Spectrum Evolution and Massive Object Formation
- 5.4. Comparative Analysis Across Gas Fractions

Chapter 6

Discussion and Conclusions

- 6.1. Interpretation of Gas-Induced Enhancements
- 6.2. Implications for SMBH Seed Formation
- 6.3. Limitations and Future Work

References

- Aarseth, S. J. (1985). Direct methods for n-body simulations. In Brackbill, J. U. and Cohen, B. I., editors, *Multiple Time Scales*, pages 377–418. Academic Press.
- Barnes, J. and Hut, P. (1986). A hierarchical $\mathcal{O}(n \log n)$ force-calculation algorithm. *nature*, 324(6096):446–449.
- Gerritsen, J., Icke, V., et al. (1997). Star formation in n-body simulation, i. *Astronomy & Astrophysics*, 325.
- Gingold, R. A. and Monaghan, J. J. (1977). Smoothed particle hydrodynamics: theory and application to non-spherical stars. *Monthly notices of the royal astronomical society*, 181(3):375–389.
- Lucy, L. B. (1977). A numerical approach to the testing of the fission hypothesis. *Astronomical Journal, vol. 82, Dec. 1977, p. 1013-1024.*, 82:1013–1024.
- Makino, J. and Aarseth, S. J. (1992). On a hermite integrator with ahmad-cohen scheme for gravitational many-body problems. *Publications of the Astronomical Society of Japan*, 44(2):141–151.
- Pelupessy, F. I. (2005). *Numerical studies of the interstellar medium on galactic scales*. PhD thesis, éditeur non identifié.
- Rasio, F. A. (2000). Particle methods in astrophysical fluid dynamics. *Progress of Theoretical Physics Supplement*, 138:609–621.
- Salmon, J. K. and Warren, M. S. (1994). Skeletons from the treecode closet. *Journal of Computational Physics*, 111(1):136–155.
- Springel, V. and Hernquist, L. (2002). Cosmological smoothed particle hydrodynamics simulations: the entropy equation. *Monthly Notices of the Royal Astronomical Society*, 333(3):649–664.
- Sweatman, W. L. (1993). A study of Lagrangian radii oscillations and core-wandering using N-body simulations. *MNRAS*, 261(3):497–512.
- Zwart, S. P. and McMillan, S. (2018). *Astrophysical Recipes: the art of AMUSE*. IOP Publishing.

Appendices

Appendix A. Fourth-Order Hermite Integration Scheme

The N-body code used in this work, **ph4**, is based on a fourth-order Hermite integrator. The following subsections describe in detail the individual time step scheme (ITS) from Makino and Aarseth (1992), including the time step criterion in the N-body code.

A.1. Step 1: Particle selection

The first step is to select the next particle to be advanced. At any given time, each particle j has its own mass m_j , time t_j , time step Δt_j , coordinates \mathbf{x}_j and \mathbf{v}_j , acceleration \mathbf{a}_j and jerk $\dot{\mathbf{a}}_j$ (with $\dot{\mathbf{a}}_j = \partial \mathbf{a}_j / \partial t$). The selected particle i is the one satisfying the condition:

$$i = \arg \min_j (t_j + \Delta t_j) \quad (\text{A.1})$$

Note that always $t_j \leq t_i + \Delta t_i$, for all j . The current simulation time is then set to $t = t_i + \Delta t_i$.

A.2. Step 2: Calculate the predicted position and velocities for all particles

The positions and velocities of all particles are predicted at time t , using a Taylor expansion up to third-order (jerk):

$$\mathbf{x}_{p,j} = \mathbf{x}_j + \mathbf{v}_j(t - t_j) + \frac{\mathbf{a}_{0,j}}{2!}(t - t_j)^2 + \frac{\dot{\mathbf{a}}_{0,j}}{3!}(t - t_j)^3 \quad (\text{A.2})$$

$$\mathbf{v}_{p,j} = \mathbf{v}_j + \mathbf{a}_{0,j}(t - t_j) + \frac{\dot{\mathbf{a}}_{0,j}}{2!}(t - t_j)^2 \quad (\text{A.3})$$

The acceleration is due only to gravitational force. The expression for each particle j is:

$$\mathbf{a}_{0,j} = \sum_{k \neq j} Gm_k \frac{\mathbf{r}_{0,jk}}{(\mathbf{r}_{0,jk}^2 + \epsilon^2)^{3/2}} \quad (\text{A.4})$$

where ϵ is the softening parameter, and

$$\mathbf{r}_{0,jk} = \mathbf{r}_k - \mathbf{r}_j \quad (\text{A.5})$$

Differentiating Eq. (A.4) with respect to time yields the jerk:

$$\dot{\mathbf{a}}_{0,j} = \frac{\partial \mathbf{a}_j}{\partial t} \quad (\text{A.6})$$

$$= \sum_{k \neq j} Gm_k \frac{\partial}{\partial t} \frac{\mathbf{r}_{0,jk}}{(\mathbf{r}_{0,jk}^2 + \epsilon^2)^{3/2}} \quad (\text{A.7})$$

$$\dot{\mathbf{a}}_{0,j} = \sum_{k \neq j} Gm_k \left[\frac{\mathbf{v}_{0,jk}}{(\mathbf{r}_{0,jk}^2 + \epsilon^2)^{3/2}} - \frac{3(\mathbf{v}_{0,jk} \cdot \mathbf{r}_{0,jk})\mathbf{r}_{0,jk}}{(\mathbf{r}_{0,jk}^2 + \epsilon^2)^{5/2}} \right] \quad (\text{A.8})$$

where

$$\mathbf{v}_{0,jk} = \mathbf{v}_k - \mathbf{v}_j \quad (\text{A.9})$$

A.3. Step 3: Calculate acceleration and jerk for particle i

Similar to equations (A.4) and (A.8), the acceleration and jerk are calculated using the predicted positions and velocity:

$$\mathbf{a}_{1,i} = \sum_{j \neq i} Gm_j \frac{\mathbf{r}_{ij}}{(\mathbf{r}_{ij}^2 + \epsilon^2)^{3/2}} \quad (\text{A.10})$$

$$\dot{\mathbf{a}}_{1,i} = \sum_{j \neq i} Gm_j \left[\frac{\mathbf{v}_{ij}}{(\mathbf{r}_{ij}^2 + \epsilon^2)^{3/2}} - \frac{3(\mathbf{v}_{ij} \cdot \mathbf{r}_{ij})\mathbf{r}_{ij}}{(\mathbf{r}_{ij}^2 + \epsilon^2)^{5/2}} \right] \quad (\text{A.11})$$

$$\mathbf{r}_{ij} = \mathbf{r}_{p,j} - \mathbf{r}_{p,i} \quad (\text{A.12})$$

$$\mathbf{v}_{ij} = \mathbf{v}_{p,j} - \mathbf{v}_{p,i} \quad (\text{A.13})$$

In this notation, the subscript 0 denotes quantities evaluated at the beginning of the time step (t_j), while the subscript 1 denotes quantities evaluated at the end of the time step (t), using the predicted position and velocity ($\mathbf{x}_{p,i}$ and $\mathbf{v}_{p,i}$).

A.4. Step 4: Second and third time derivative of acceleration, using Hermite interpolation

To obtain a high-order correction of \mathbf{x} and \mathbf{v} , the acceleration of particle i is modeled as a third-order polynomial in time:

$$\mathbf{a}(\tau) = \alpha\tau^3 + \beta\tau^2 + \gamma\tau + \delta \quad (\text{A.14})$$

The successive time derivatives of $\mathbf{a}(\tau)$ are then:

$$\dot{\mathbf{a}}(\tau) = 3\alpha\tau^2 + 2\beta\tau + \gamma \quad (\text{A.15})$$

$$\mathbf{a}^{(2)}(\tau) = 6\alpha\tau + 2\beta \quad (\text{A.16})$$

$$\mathbf{a}^{(3)}(\tau) = 6\alpha \quad (\text{A.17})$$

The coefficients α , β , γ , and δ are determined by using the known values of acceleration and jerk at times t_i and t . This provides a system of four equations:

$$\mathbf{a}(t_i) = \mathbf{a}_{0,i} = \alpha t_i^3 + \beta t_i^2 + \gamma t_i + \delta \quad (\text{A.18})$$

$$\mathbf{a}(t) = \mathbf{a}_{1,i} = \alpha t^3 + \beta t^2 + \gamma t + \delta \quad (\text{A.19})$$

$$\dot{\mathbf{a}}(t_i) = \dot{\mathbf{a}}_{0,i} = 3\alpha t_i^2 + 2\beta t_i + \gamma \quad (\text{A.20})$$

$$\dot{\mathbf{a}}(t) = \dot{\mathbf{a}}_{1,i} = 3\alpha t^2 + 2\beta t + \gamma \quad (\text{A.21})$$

where $t = t_i + \Delta t_i$ is the current time. As the system of equations is linearly independent, the four coefficients can be determined. However, determining α and β is enough to get the second and third time derivative of acceleration. From (A.21):

$$\gamma = \dot{\mathbf{a}}_{1,i} - 3\alpha t^2 - 2\beta t \quad (\text{A.22})$$

Subtracting Eq. (A.20) from (A.21):

$$\beta = \frac{(\dot{\mathbf{a}}_{1,i} - \dot{\mathbf{a}}_{0,i}) - \alpha 3(t^2 - t_i^2)}{2(t - t_i)} \quad (\text{A.23})$$

Subtracting Eq. (A.18) from (A.19), and using results from (A.22) and (A.23) gives an expression for α :

$$\alpha = \frac{(\dot{\mathbf{a}}_{1,i} + \dot{\mathbf{a}}_{0,i})(t - t_i) - 2(\mathbf{a}_{1,i} - \mathbf{a}_{0,i})}{(t - t_i)^3} \quad (\text{A.24})$$

Replacing this result in Eq. (A.23):

$$\beta = \frac{-\dot{\mathbf{a}}_{1,i}(t + 2t_i) - \dot{\mathbf{a}}_{0,i}(2t + t_i)}{(t - t_i)^2} + \frac{3(\mathbf{a}_{1,i} - \mathbf{a}_{0,i})(t + t_i)}{(t - t_i)^3} \quad (\text{A.25})$$

The second and third time derivatives of the acceleration at time t_i can now be evaluated. For the Eq. (A.17), and using $t - t_i = \Delta t_i$:

$$\mathbf{a}_{0,i}^{(3)} = \mathbf{a}^{(3)}(t_i) = 6\alpha \quad (\text{A.26})$$

$$\mathbf{a}_{0,i}^{(3)} = 6 \frac{(\dot{\mathbf{a}}_{1,i} + \dot{\mathbf{a}}_{0,i})\Delta t_i - 2(\mathbf{a}_{1,i} - \mathbf{a}_{0,i})}{\Delta t_i^3} \quad (\text{A.27})$$

$$\mathbf{a}_{0,i}^{(3)} = \frac{12(\mathbf{a}_{0,i} - \mathbf{a}_{1,i}) + 6(\dot{\mathbf{a}}_{0,i} + \dot{\mathbf{a}}_{1,i})\Delta t_i}{\Delta t_i^3} \quad (\text{A.28})$$

Evaluating the second time derivative in t_i , and replacing the obtained for α and β :

$$\mathbf{a}_{0,i}^{(2)} = \mathbf{a}^{(2)}(t_i) = 6\alpha t_i + \beta \quad (\text{A.29})$$

$$\mathbf{a}_{0,i}^{(2)} = \frac{-6(\mathbf{a}_{0,i} - \mathbf{a}_{1,i}) - \Delta t_i(4\dot{\mathbf{a}}_{0,i} + 2\dot{\mathbf{a}}_{1,i})}{\Delta t_i^2} \quad (\text{A.30})$$

A.5. Step 5: Add corrections

The next step in the scheme is to correct position and velocity of particle i at time t . Using a higher-order Taylor expansion around t_i :

$$\mathbf{x}_i(t_i + \Delta t_i) = \mathbf{x}_i(t_i) + \dot{\mathbf{x}}_i(t_i)\Delta t_i + \frac{\mathbf{x}_i^{(2)}(t_i)\Delta t_i^2}{2!} + \dots + \frac{\mathbf{x}_i^{(5)}(t_i)\Delta t_i^5}{5!} \quad (\text{A.31})$$

$$= \mathbf{x}_i + \mathbf{v}_i\Delta t_i + \frac{\mathbf{a}_{0,i}\Delta t_i^2}{2} + \frac{\dot{\mathbf{a}}_{0,i}\Delta t_i^3}{6} + \frac{\mathbf{a}_{0,i}^{(2)}\Delta t_i^4}{24} + \frac{\mathbf{a}_{0,i}^{(3)}\Delta t_i^5}{120} \quad (\text{A.32})$$

The first four terms of this expansion correspond to the predicted position $\mathbf{x}_{p,i}$ from Eq. (A.2). Therefore, the corrected position can be written as:

$$\mathbf{x}_i(t_i + \Delta t_i) = \mathbf{x}_{p,i} + \frac{\mathbf{a}_{0,i}^{(2)}\Delta t_i^4}{24} + \frac{\mathbf{a}_{0,i}^{(3)}\Delta t_i^5}{120} \quad (\text{A.33})$$

In a similar way, the corrected velocity is:

$$\mathbf{v}_i(t_i + \Delta t_i) = \mathbf{v}_{p,i} + \frac{\mathbf{a}_{0,i}^{(2)}\Delta t_i^3}{6} + \frac{\mathbf{a}_{0,i}^{(3)}\Delta t_i^4}{24} \quad (\text{A.34})$$

The advantage of this scheme is that achieving high integration accuracy only requires the explicit calculation of the acceleration and jerk for all particles, and the predicted acceleration and jerk for the particle being advanced. This results in an integration scheme that is fourth-order accurate in time ($\mathcal{O}(a^{(3)})$).

A.6. Step 6: Time step update

After updating the position and velocity of particle i , a new time step Δt_i must be calculated. This step is crucial for controlling the integration error. A proven and stable criterion is given by the standard formula Aarseth (1985):

$$\Delta t_i = \sqrt{\eta \frac{|\mathbf{a}_{1,i}| |\mathbf{a}_{1,i}^{(2)}| + |\dot{\mathbf{a}}_{1,i}|^2}{|\dot{\mathbf{a}}_{1,i}| |\mathbf{a}_{1,i}^{(3)}| + |\mathbf{a}_{1,i}^{(2)}|^2}} \quad (\text{A.35})$$

The values for $\mathbf{a}_{1,i}$ and $\dot{\mathbf{a}}_{1,i}$ are known from the direct calculation in Step 3. The value of $\mathbf{a}^{(3)}(t)$ is constant, since a third-order polynomial interpolation is used. Only $\mathbf{a}_{1,i}^{(2)}$ should be calculated:

$$\mathbf{a}_{1,i}^{(2)} = \mathbf{a}_{0,i}^{(2)} + \Delta t_i \mathbf{a}_{0,i}^{(3)} \quad (\text{A.36})$$

During the initialization of the algorithm, the higher-order derivatives of the acceleration are not available, so an alternative formula for time step can be used in the startup:

$$\Delta t = \eta_s \frac{|\mathbf{a}|}{|\dot{\mathbf{a}}|} \quad (\text{A.37})$$

The suggested value for the startup parameter is $\eta_s \sim 0.01$ Makino and Aarseth (1992).